INFLUENCE OF THE NUMBER OF ROTOR BLADES ON HELICOPTER ACTIVE VIBRATION REDUCTION POTENTIAL

Thomas Mannchen, Klaus H. Well
Institute of Flight Mechanics and Control, University of Stuttgart
Pfaffenwaldring 7a, 70550 Stuttgart, Germany
www.ifr.uni-stuttgart.de

Abstract

This paper discusses the time-periodicity of the helicopter rotor in forward flight and its effects on the design of control laws for vibration reduction and damping enhancement using individual blade control. The extent to which the achievable vibration reduction depends on the number of degrees of freedom is analyzed. Therefore, a simple analytical model of an N-blade helicopter rotor is developed. In order to assess the influence of the number of blades on the vibration reduction potential, various controllers are designed for rotors with different numbers of blades. The capability of an observer-based control law to increase lag damping without using dedicated blade sensors is demonstrated via simulation with a comprehensive aeromechanical model of a four-blade BO 105 helicopter rotor derived with Camrad II.

Nomenclature

a	Blade section lift-curve slope
A, B, C, D	State-space matrices
c	Blade chord
C	Damping coefficient (with subscript)
d	Disturbance vector
e	Hinge offset
F	Force (with subscript)
I	Generalized mass (with subscript) Moment of inertia (with subscript)
K	Gain matrix Spring constant (with subscript)
m	Blade index
M	Moment (with subscript)
n	Harmonic index
N	Blade root moment (with subscript) Number of rotor blades
r	Reference vector
R	Rotor radius
S	Shear force (with subscript)
v	Control deviation vector
x, y, u	State, output, input vectors
β	Blade flap angle
γ	Blade lock number
ζ	Blade lag angle
θ	Blade pitch angle
ν	Rotating natural frequency (with subscript)
ρ	Air density
ψ	Azimuth angle Dimensionless time variable
Ω	Rotor rotational frequency
0, $1c$, $1s$, nc, ns, d	Degrees of freedom of the Fourier coordinate transformation
(1), …, (N)	Blade degrees of freedom
/rev	Frequency unit: per rotor revolution
$\dot{(\,)}$	$d(\,)/d\psi$

Introduction

Helicopter suffer from high vibration. This vibration is mostly caused by the main rotor, which operates in a complex aerodynamic flow field. Changing aerodynamic effects, pilot inputs via the swashplate, and interactions of blades and vortices of preceding blades are causes of oscillations in the flexible rotor blades which are transmitted through the rotor hub and cause vibration in the fuselage. Fuselage vibration leads to human discomfort and fatigue damage of structural components which both give reason to the aim of helicopter vibration reduction.

Concepts for active vibration control are higher harmonic control (HHC) and individual blade control (IBC). Both methods aim at inducing additional forces and moments at the rotor which are opposite in phase and equal in amplitude with the original forces and moments, leading to destructive interference. The original vibration is consequently

Presented at the 28th European Rotorcraft Forum, 17-20 September 2002, Bristol, UK, Paper No. 81

reduced and ideally canceled out. By IBC, the blades are individually controlled in the rotating frame above the swashplate. In the concept of individual blade *root* control, the lift of the blade is varied by changing the pitch of the blade at its root. Therefore the pitch link rods are substituted by hydraulic actuators allowing a blade pitch control superimposed to the swashplate commands. A four-blade BO 105 helicopter equipped with an individual blade root control system is considered here (Ref. 15).

One advantage of individual blade root control over other individual blade control concepts via flaps, twist, etc., is that no changes to the blade are necessary. Thus, the blades do not need to be recertified. However, if the original blades are used, no blade sensors are available and, consequently, no measurements are available in the rotating frame. The availability of only hub load (and possibly fuselage) sensors imposes certain restrictions on the design of the control law, which this paper seeks to examine.

Helicopter vibration reduction belongs to the class of vibration control problems for plants with periodic coefficients. Here, periodicity is a result of the mechanics of the system and cannot be avoided. A linear time-periodic system responds to a sinusoidal input not only with a sinusoid at the excitation frequency, as linear time-constant systems do, but also at additional harmonic frequencies that are spaced by multiples of the plant-periodic frequency (Ref. 2). The introduction of multiblade coordinates (MBC, Ref. 6) opens up the possibility of using a wide range of time-invariant controller synthesis techniques, since the periodicity of the plant is (partly) preserved in a time-constant MBC representation. This paper addresses effects associated with the time-periodicity and examines the interaction of the multiblade coordinate transformation, the multiharmonic response of the system, and the hub filtering effect of the rotor.

An elementary issue in helicopter vibration control is the selection of outputs to be controlled. For a four-blade rotor, typically three hub forces/moments are chosen, e.g. the force vector or a combination of the force in thrust direction and the roll and pitch moment. However, a reduction of vibration in selected hub loads can lead to reduced or increased vibration in the remaining hub loads, depending on the dynamic properties of the system, but typically vibration is increased in outputs not considered for vibration reduction, which is obviously counter-productive to the aim of reducing vibration that is transmitted to the fuselage. This paper examines the extent to which the achievable vibration reduction depends on the number of degrees of freedom and presents a systematic analysis of the extent to which the number of degrees of freedom available for vibration reduction depends on the number of rotor blades.

The paper is organized as follows. Firstly, the models used for analysis and design are described, followed by a presentation of the effects associated with periodicity. Next, vibration reduction results are presented, and lag damping enhancement is discussed. Finally, some conclusions are presented.

Model Description

In this section, two different rotor models are presented: a simple analytical model and a complex aeromechanical analysis model, including advanced rotor aerodynamics in addition to detailed kinematics and detailed dynamics derived with the commercial helicopter analysis software Camrad II (Ref. 7).

Analytical Rotor Model

An analytical model of an N-blade helicopter rotor is developed. The model is outlined briefly in this section. For a detailed derivation see Ref. 10, Ref. 14, and the original source Ref. 8. The structure of the rotor blades is modelled using mass and spring systems. In aerodynamics, blade element theory is used to determine the blade loading. Only rigid flap and lag motion is considered, with collective, cyclic, and, in case of even blade numbers, differential pitch control. The rotor is articulated with flap and lag hinge offsets. In general, small angles are assumed. The section aerodynamic characteristics are described by a constant lift curve slope and a mean profile drag coefficient. The effects of stall, compressibility, and radial flow are not included. A uniform induced velocity is used. The blade has constant chord and linear twist. Higher harmonics of flap and lag motion and the pitch degrees of freedom are neglected. The model parameters are chosen to resemble those of the BO 105 helicopter.

While the basic features of rotor behavior are contained in the model described above, it is far too limited for accurate quantitative results. Despite the fact that various effects are neglected and that structural and aerodynamic modelling is far too simple to predict vibrational loads, the model is assumed to allow a qualitative evaluation of the potential to influence vibration with IBC from a control law design perspective.

The motion of a hinged blade (“articulated rotor”) consists basically of rigid body rotation about each hinge, with restoring moments as a result of the centrifugal forces acting on the rotating blade. For a blade without hinges (“hingeless rotor”), the funda-

mental modes of out-of-plane and in-plane bending define the flap and lag motion. Because of the high centrifugal stiffening of the blade, these modes are similar to and can be approximated by the rigid body rotations of hinged blades, except in the vicinity of the root, where most of the bending takes place (Ref. 8). In addition to the flap and lag motion, it is possible to change the pitch of the blade in order to control the rotor. Pitch motion allows the angle of attack of the blade to be controlled and hence the aerodynamic forces on the rotor.

The forces acting on the blade are the inertial, centrifugal, Coriolis, and aerodynamic forces. Equilibrium of moments about the flap hinge (with hinge offset e), including a spring moment $K_\beta(\beta - \beta_p)$ with the precone angle β_p, gives the flap equation of motion expressed in dimensionless quantities

$$I_\beta^*(\ddot{\beta} + \nu_\beta^2\beta) - 2I_{\beta\zeta}^*\beta\dot{\zeta} = \frac{K_\beta\beta_p}{I_b(1-e)\Omega^2} + \gamma M_F \qquad (1)$$

with the natural frequency of the flap motion

$$\nu_\beta^2 = 1 + \frac{3e}{2(1-e)} + \frac{K_\beta}{\Omega^2 I_b(1-e)^2} \qquad (2)$$

the normalized generalized mass of the flap mode $I_\beta^* = 1 - e$, the normalized Coriolis flap-lag coupling $I_{\beta\zeta}^* = 1$, the blade lock number

$$\gamma = \frac{\rho acR^4}{I_b} \qquad (3)$$

where ρ is the air density, a the blade section lift-curve slope, c the blade chord, I_b the characteristic inertia of the rotor blade, and M_F the aerodynamic flap moment, which is mainly a function of helicopter flight speed V, thrust T, and pitch control input θ_{con}, see Ref. 10, Ref. 14, and Ref. 8.

Equilibrium of moments about the lag hinge, including a spring moment $K_\zeta\zeta$ and a mechanical lag damper term $C_\zeta^*\dot{\zeta}$, gives the lag equation of motion that is expressed in dimensionless quantities as:

$$I_\zeta^*(\ddot{\zeta} + \nu_\zeta^2\zeta) + 2I_{\beta\zeta}^*\beta\dot{\beta} + C_\zeta^*\dot{\zeta} = \gamma M_L \qquad (4)$$

The natural frequency of the lag motion is

$$\nu_\zeta^2 = \frac{3e}{2(1-e)} + \frac{K_\zeta}{\Omega^2 I_b(1-e)^2} \qquad (5)$$

and the normalized generalized mass of the lag mode is $I_\zeta^* = 1 - e$. The aerodynamic lag moment M_L is again a function of flight speed, thrust, and pitch control input, see Ref. 10, Ref. 14, and Ref. 8.

Loads, Vibrations, and Hub Filtering

The forces and moments at the root of the rotating blades are transmitted to the helicopter airframe. The steady components of these hub reactions in the nonrotating frame are the forces and moments required to trim the helicopter. The higher frequency components cause helicopter vibration. Fig. 1 shows the definition of the root shears and moments of the rotating blade and the forces and moments acting on the hub in the nonrotating frame.

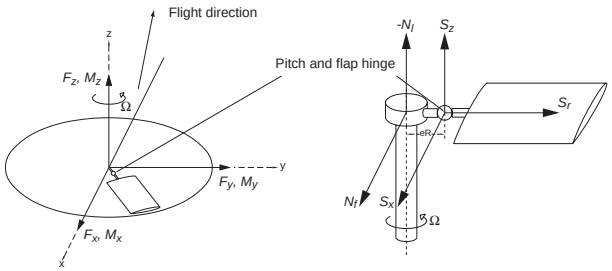

Fig. 1 Forces and moments in the nonrotating and rotating system (Ref. 10, Ref. 8)

The vertical shear force S_z generates the rotor thrust F_z and the in-plane shear forces S_x and S_r cause the rotor side and drag forces F_y and F_x. The flapwise root moment N_F produces the rotor pitch and roll moments M_y and M_x, whereas the lagwise moment N_L results in the rotor shaft torque $-M_z$. The rotating blade root loads can be obtained by integrating the section forces acting on the blades. The forces and moments in the nonrotating frame are obtained by summing over all N blades, where the notation $^{(m)}$ stands for the m^{th} blade:

$$F_x = \sum_{m=1}^{N} (S_r^{(m)}\cos\psi_m + S_x^{(m)}\sin\psi_m) \qquad (6)$$

$$F_y = \sum_{m=1}^{N} (S_r^{(m)}\sin\psi_m - S_x^{(m)}\cos\psi_m) \qquad (7)$$

$$F_z = \sum_{m=1}^{N} S_z^{(m)} \qquad (8)$$

$$M_x = \sum_{m=1}^{N} N_f^{(m)}\sin\psi_m \qquad (9)$$

$$M_y = -\sum_{m=1}^{N} N_f^{(m)}\cos\psi_m \qquad (10)$$

$$M_z = -\sum_{m=1}^{N} N_l^{(m)} \qquad (11)$$

In steady-state forward flight, the root reaction of the m^{th} blade ($m = 1, \ldots, N$) is a periodic function of $\psi_m = \psi + m\Delta\psi$ with $\Delta\psi = 2\pi/N$. Therefore, all

blades have identical loading and motion. When the loads are written in the rotating frame as Fourier series and the summations are evaluated, all loads cancel at the rotor hub, except for those appearing in the nonrotating frame as harmonics of pN/rev (Ref. 8). The rotor hub basically acts as a filter, transmitting to the helicopter only harmonics of the rotor forces at integer multiples p of N/rev. Table 1 summarizes the transmission of loads through the rotor hub.

Table 1 Transmission of helicopter vibration through the rotor hub (Ref. 8)

Nonrotating Frame		**Rotating Frame**
Thrust at pN/rev	from	vertical shear at pN/rev
Torque at pN/rev	from	lagwise moment at pN/rev
Rotor drag and side forces at pN/rev	from	in-plane shears at $pN\pm1$/rev
Pitch and roll moments at pN/rev	from	flapwise moments at $pN\pm1$/rev

Multiblade Coordinate Transformation

The equations of motion are derived in the rotating frame. However, the rotor responds as a whole to excitations (control inputs, gusts) from the nonrotating frame. This is the motivation to use coordinates in the nonrotating frame. Multiblade coordinates (MBC), which result from a linear Fourier coordinate transformation from single blade coordinates (SBC), are introduced (Ref. 6). The following equations describe the transformation from SBC to MBC. As an example, the flap motion is considered. $\beta^{(1)} \ldots \beta^{(N)}$ denote the flap angles in SBC, whereas the coordinates β_0 (collective mode), β_{nc} and β_{ns} (cosine and the sine modes), and β_d (differential mode, exists only for N even) are used in MBC. The blade index m ranges from 1 to N. The azimuth is $\psi_m = \psi + m \cdot \Delta\psi$ with the dimensionless time variable $\psi = \Omega t$ for constant rotational speed Ω and the equal azimuthal spacing between the blades $\Delta\psi = 2\pi/N$.

$$\beta_0 = \frac{1}{N} \sum_{m=1}^{N} \beta^{(m)} \tag{12}$$

$$\beta_{nc} = \frac{2}{N} \sum_{m=1}^{N} \beta^{(m)} \cos n\psi_m \tag{13}$$

$$\beta_{ns} = \frac{2}{N} \sum_{m=1}^{N} \beta^{(m)} \sin n\psi_m \tag{14}$$

$$\beta_d = \frac{1}{N} \sum_{m=1}^{N} \beta^{(m)} (-1)^m \tag{15}$$

The inverse coordinate transformation is given by:

$$\beta^{(m)} = \beta_0 + \sum_n (\beta_{nc} \cos n\psi_m + \beta_{ns} \sin n\psi_m) + \beta_d (-1)^m \tag{16}$$

The summation index n goes from 1 to $(N-1)/2$ for N odd and from 1 to $(N-2)/2$ for N even.

Trimming and Linearization

Linearization is typically performed about an operating condition, e.g. a trim state x^* and trim input u^*. Here, the system is linearized about a trim *trajectory* over one rotor revolution, resulting in a linear time-periodic system. The three control variables, collective, longitudinal cyclic, and lateral cyclic pitch, are adjusted to trim three quantities: thrust, propulsive force, and side force, referred to as “wind tunnel trimming”. The trim state trajectory $x^*(\psi)$ is obtained by means of nonlinear simulation and is written as a Fourier series. The trim input trajectory $u^*(\psi)$ is defined by the collective and cyclic pilot inputs.

The resulting system is transformed into state-space form:

$$\begin{aligned} \dot{x} &= A(\psi)x + B(\psi)u \\ y &= C(\psi)x + D(\psi)u \end{aligned} \tag{17}$$

Both state and input vectors are given in MBC:

$$x = [\dot{\beta}_0, \dot{\beta}_{nc}, \dot{\beta}_{ns}, \dot{\beta}_d, \dot{\zeta}_0, \dot{\zeta}_{nc}, \dot{\zeta}_{ns}, \dot{\zeta}_d, \beta_0, \beta_{nc}, \beta_{ns}, \beta_d, \zeta_0, \zeta_{nc}, \zeta_{ns}, \zeta_d]^T \tag{18}$$

$$u = [\theta_0, \theta_{nc}, \theta_{ns}, \theta_d]^T \tag{19}$$

The harmonic index n goes from $n = 1$ to $(N-1)/2$ for N odd and from $n = 1$ to $(N-2)/2$ for N even. The differential degree of freedom (index d) only exists if N is even.

The output vector contains the hub loads in the nonrotating system:

$$y = [F_x, F_y, F_z, M_x, M_y, M_z]^T \tag{20}$$

Camrad II Rotor Model

The aeromechanical analysis software Camrad II (Ref. 7) is used to derive a state-space model of a BO 105 helicopter rotor with four flexible blades (Ref. 4). This model very much resembles the simple analytical model in the previous section in terms of inputs and outputs, as well as in terms of time-

periodicity and multiblade coordinates, but is of much higher complexity and accuracy, thus allowing quantitative results.

The rotor blades are modelled as beams by finite elements, allowing flap (out-of-plane), lag (in-plane), and torsion motion. Aerodynamics are calculated using blade element theory combined with experimental airfoil tables and a wake model. The structural blade modes considered are four flap modes, two lag modes, and the first torsion mode. Higher frequency structural and aerodynamical modes, as well as flight mechanical modes are neglected. The BO 105 helicopter fuselage is implemented as a rigid body in order to model the inertial properties of the helicopter. Aerodynamic effects of the fuselage and stabilizer are considered by table data. The tail rotor is treated as a rigid rotor without degrees of freedom. The actuators are modelled using first-order dynamics.

Periodicity

This section presents aspects of the plant that arise from its periodicity and discusses some consequences for control law design. The interplay of the Fourier coordinate transformation, the multiharmonic response of the periodic plant, and the hub filtering effect of the rotor are analyzed in detail.

Multiharmonic Responses

An ordinary time-constant linear system, described with one or a set of linear differential equations with constant coefficients, responds to a single harmonic input with a single harmonic output of the same frequency. A system that can also be described with one or a set of linear differential equations having time-periodic coefficients is called a “linear time-periodic system”. The response of a linear time-periodic system to a single harmonic input is generally a multiharmonic output. The Fourier coefficients of the multiharmonic response depend on the system properties, i.e. on the periodicity of the coefficients of its differential equations. Fig. 2 illustrates the fundamental difference between time-constant and time-periodic linear systems.

Transmissibility of Single Harmonic Blade Inputs

The following analysis is based on the time-periodic Camrad II model of the four-blade BO 105 helicopter in forward flight (Ref. 4). Open-loop simulations are performed with various single harmonic sinusoidal inputs with various frequencies but identical amplitudes of $1°$. The bar graphs in Fig. 3 represent the output amplitude of the Fourier coefficients

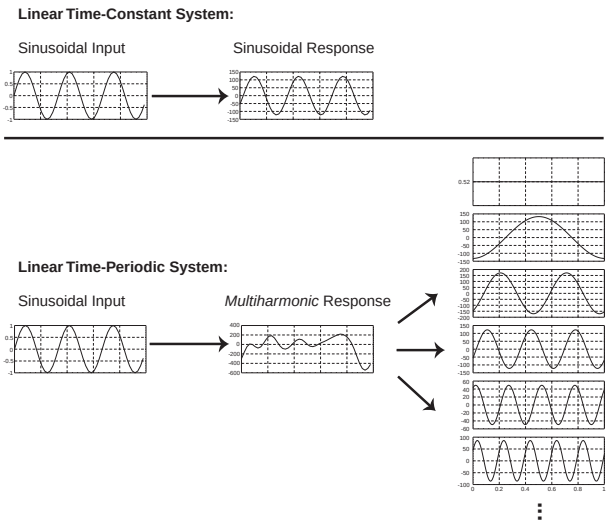

Fig. 2 Multiharmonic response of a linear time-periodic system to a single harmonic input (Ref. 9)

and correspond to the input frequencies of 2/rev to 6/rev. The amplitudes are given for different outputs: blade root moments for one blade in the rotating frame and rotor hub loads in the nonrotating frame. The Fourier coefficients are given for frequencies from 0/rev to 8/rev. Note that the multiharmonic responses of the plant to the single harmonic input are caused by the time-periodic coefficients of the system, as described in the previous section. The input of the m^{th} blade ($m = 1$ to N) is a periodic function of $\psi_m = \psi + m\Delta\psi$, $\Delta\psi = 2\pi/N$. Therefore, all blades have identical loading and motion.

The blade root load outputs in the rotating frame respond to a single harmonic input with a multiharmonic output generally in all frequencies (only limited by the periodicity of the system). However, the response is dominated by frequencies close by, e.g. the response of a 2/rev input is typically dominated by 1/rev, 2/rev, and 3/rev sinusoidal components. The largest output amplitude is typically in the frequency of the input, whereas the amplitude of the “sidebands”, i.e. the responses in frequencies different from the input frequency, typically decrease as the difference in frequency increases.

Fig. 4 shows the same simulation, but now with the time-constant rotor model in MBC. The rotating blade root outputs respond to single harmonic inputs with the frequencies 2/rev only with single harmonic outputs of 2/rev. The same also holds for 6/rev inputs. By means of multiblade coordinates, the system responds to inputs with frequencies of 3/rev, 4/rev, and 5/rev, with multiharmonic outputs in *all* three frequencies 3/rev, 4/rev, and 5/rev, respectively. This is due to the fact that the multiblade coordinate transformation for the four-

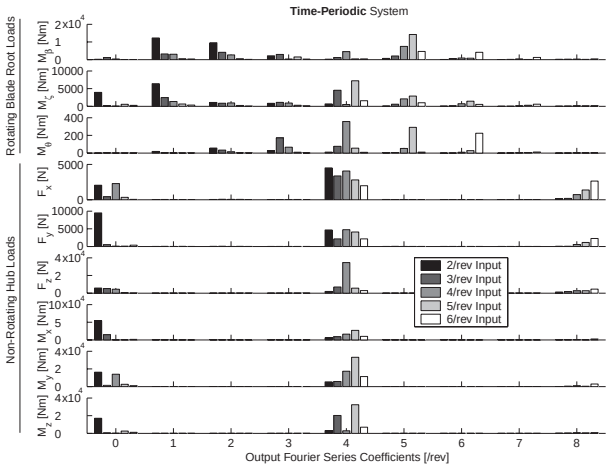

Fig. 3 Multiharmonic response of the periodic system at the blade root (rotating system) and at the hub (nonrotating system) to single harmonic inputs

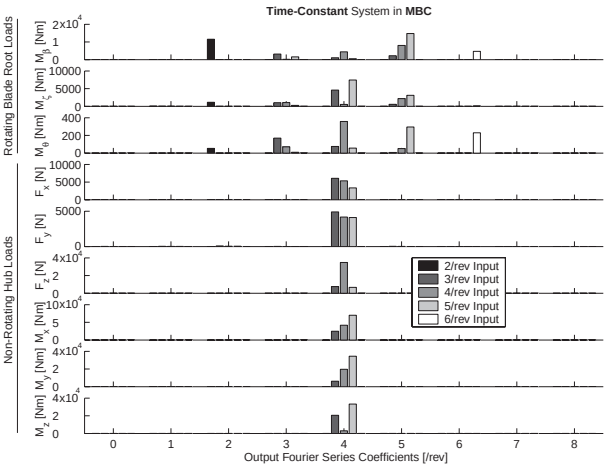

Fig. 4 Multiharmonic response of the constant system in MBC at the blade root (rotating system) and at the hub (nonrotating system) to single harmonic inputs

blade rotor introduces a progressive $(4+1)$/rev $= 5$/rev and a regressive $(4-1)$/rev $= 3$/rev cyclic mode. The multiharmonic response of the time-constant plant demonstrates how the transformation from SBC to MBC (partly) preserves the periodicity of the plant.

Hub Filtering

In order to determine the total influence of a rotor with N blades undergoing identical periodic motion, it is necessary to evaluate sums of harmonics, e.g.

$$\frac{1}{N}\sum_{m=1}^{N} \sin n\psi_m = f_n \sin n\psi \qquad (21)$$

where $f_n = 1$ only if n is a multiple of the number of blades, otherwise $f_n = 0$ (Ref. 8). Again, the azimuth of the m^{th} blade is given by $\psi_m = \psi + m\Delta\psi$, $\Delta\psi = 2\pi/\mathrm{N}$. This means that blade root loads with a frequency of N/rev are transmitted to the nonrotating frame. However, there are blade root loads that are multiplied by terms $\sin\psi_m$ (or $\cos\psi$), see (6), (7), (9), (10). By means of trigonometric relations, e.g.

$$\sin x \cdot \sin y = \frac{1}{2}(\cos(x-y) - \cos(x+y)) \qquad (22)$$

it can be shown that $(N-1)$/rev, N/rev, and $(N+1)$/rev blade root loads yield N/rev terms in the summation and consequently are transmitted through the hub to the nonrotating system, see Table 1.

As regards transmission from individual blade commands in SBC to nonrotating hub loads, it can be stated that, in the periodic system, inputs of *any* frequency causing $(N-1)$/rev, N/rev, or $(N+1)$/rev blade root loads are transmitted to the rotor hub. Consequently, for a four-blade rotor, not only 3/rev, 4/rev, and 5/rev inputs, but also 2/rev and 6/rev inputs can be used to provoke 4/rev hub loads in the nonrotating system. However, whereas the 3/rev, 4/rev, and 5/rev inputs are "directly" transmitted to the rotor hub, the 2/rev and 6/rev inputs are only transmitted "indirectly" via the multiharmonic sideband responses of the blade root loads. These theoretical results are confirmed by experiments in Ref. 13.

Unfortunately, the Fourier coordinate transformation for the four-blade rotor translates 4/rev MBC inputs only into 3/rev, 4/rev, and 5/rev individual blade commands in SBC, leaving the 2/rev and 6/rev inputs inaccessible for controller designs based on a time-constant model. In contrast to this, periodic controllers based on the periodic plant can make use of the additional input frequencies; Ref. 11 shows an example of where a periodic controller uses a 2/rev input. However, there are two drawbacks of 2/rev and 6/rev inputs: First, the effectiveness is reduced in comparison to 3/rev, 4/rev, and 5/rev inputs due to "indirect" transmission via sidebands only, as also reported in Ref. 13. Second, the 2/rev input considerable affects 0/rev trim loads and the 6/rev input affects 8/rev hub loads in what could be an undesired way, see Fig. 3.

Periodicity of the Total System in MBC

The total system consists of three subsystems with periodicity effects, see Fig. 5. First, for a four-blade rotor, the 4/rev input signal in MBC is split up into 3/rev, 4/rev, and 5/rev signals in the coordinate transformation. Additional signals with $(N-2)$/rev and $(N+2)$/rev are created for rotors with $N = 5$

or 6 rotor blades[i]. The rotor blades considered to be the second subsystem respond to these input signals with multiharmonic responses. The resulting signals are dominated by frequencies of between 2/rev and 6/rev. Finally, the hub filters frequencies with integer multiples of the number of blades, i.e. 0/rev, mostly 4/rev, 8/rev, etc.

The system can be linearized from the input in MBC to the hub load output[ii]. Both signals are given in the nonrotating frame. This system can be averaged, i.e. constant coefficients can be used, neglecting higher-order Fourier series terms. The resulting system is a linear time-constant system. This opens up the possibility of using a wide range of classical linear control law synthesis methods. The single harmonic 4/rev to 4/rev transfer function of the plant internally contains the 3/rev, 4/rev, and 5/rev physical transmission paths, making it an ideal choice on which to base control law designs.

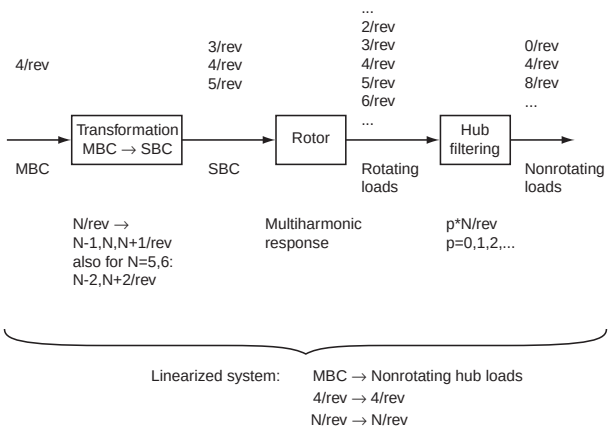

Fig. 5 Transmission of signals through the coordinate transformation, rotor, and hub

Vibration Reduction for the N-Blade Rotor

A control law for the N-blade rotor is developed in this section. The focus is on analyzing the potential of individual blade control and examining the dependence of the number of rotor blades. Optimal output feedback strategies are used to design control laws in order to reduce vibration.

N-Blade Rotor Effects

A straight forward approach to studying the influence of the number of rotor blades would be to compare different helicopters with different numbers of rotor blades. A drawback of this approach is that the results would be affected by two factors: First, by the number of blades, as intended, and second by the fact that the different helicopters might have been designed for different missions, differ in size, mass, etc., whereby the second would make comparisons difficult, if not impossible. To overcome this problem, fictitious N-blade rotors are modelled for the four-blade BO 105 helicopter. In the four-blade rotor, all parameters of the rotor model are chosen to resemble the original BO 105 helicopter. For $N \neq 4$ blade rotors, the number of blades changes. If identical blades were used to those of the $N = 4$ blade rotor, the thrust and other forces and moments produced by the rotor would change. Therefore, the blade chord is scaled by the factor $4/N$. Consequently, the lift per blade is scaled and the total thrust is approximately independent of the number of rotor blades. This leads to approximately the same trim situation, i.e. the N-blade rotors produce the same trim forces and moments at the rotor hub for a given input of pilot collective and cyclic pitch. Choosing the blade chord as a parameter to be adapted to the number of blades means that the rotational speed, the rotor diameter, and fundamental blade properties, such as the natural frequencies of the flap and lag motion, remain unchanged, which helps to simplify comparisons (Ref. 14).

The different rotor models are trimmed at identical forward cruise flight conditions and are linearized about a trajectory about one rotor revolution. The result is a family of linear time-periodic models for rotors with N blades that differ in the number of inputs (N, corresponding to N blades and N input modes in MBC) and states ($4N$, corresponding to flap and lag degrees of freedom and derivatives).

The most dominant vibration occurs at the blade passage frequency of N/rev (Ref. 4). Amplitude and phase information is only available for the four-blade rotor from calculations using Camrad II or from flight tests. For the moment, it is assumed that the amplitude and phase is independent of N and only the excitation frequency is changed. Ref. 1 gives a comparison of vibration for a four and five-blade helicopter. The results show that the amplitude of most hub loads is decreased with the five-blade rotor, except for the vertical shear in some cruise flight conditions. The above assumption is therefore simplifying. When comparing results, therefore, it has to be kept in mind that approximating N/rev vibration with 4/rev data tends to underestimate true vibration for $N < 4$ and overestimate vibration for $N > 4$.

i. In the case of $N = 7$ rotor blades, third-order cyclic modes lead to additional frequencies of $(N-3)$/rev and $(N+3)$/rev.

ii. The coordinate transformation and the rotor are not realized as a series connection as shown in Fig. 5; rather both inputs and states of the rotor are transformed to MBC.

Optimal Output Feedback Control Law Design

The objective of the control law is to cancel vibration that enters the system as an output disturbance. The pitch of the individual blades can be controlled in order to change the lift (and drag) of the blades and consequently provoke additional forces and moments at the rotor hub. By applying appropriate blade pitch commands, the baseline vibration can be reduced and ideally cancelled out at the rotor hub. The resulting hub loads are available to the controller as a measurement.

This disturbance rejection control problem is dealt with by implementing a servo-compensator. The servo-compensator is a dynamic compensator that is in resonance with the external disturbances acting on the plant (Ref. 3), representing an internal model of the external disturbances. In the helicopter vibration problem, the external disturbances of sinusoidal type with the blade passage frequency N/rev are considered. The internal model of this external disturbance is an undamped oscillator tuned to the disturbance frequency. The oscillator is implemented as a second-order notch filter.

Standard optimal output feedback strategies are used to design the control law. A system of the form

$$\begin{aligned} \dot{x} &= Ax + Bu \\ y &= Cx + Du + d \end{aligned} \tag{23}$$

is considered, whereby x is the state vector, u the input vector, y the output vector, and d the output disturbance vector. The control law has the form:

$$u = -Ky \tag{24}$$

The gain-matrix K is to be chosen to minimize the performance criterion

$$J = \int_0^\infty (x^\mathrm{T} Q x + u^\mathrm{T} R u)\, dt \tag{25}$$

where $Q = \Gamma^\mathrm{T}\Gamma$ such that (Γ, A) is detectable and $R > 0$ (Ref. 12).

The linear time-constant plant in MBC is augmented with the servo-compensator. The gain matrix is derived using an algorithm (Ref. 12) for calculating optimal output feedback gains for the augmented system. Fig. 6 shows the structure of the output feedback system with plant, servo-compensator, gain matrix, and with the baseline vibration acting on the system as output disturbances.

Vibration Reduction Results

For the family of N-blade rotors (here three to seven-blade rotors are considered), a set of controllers is designed using identical state and control weighting matrices in the performance criterion, as

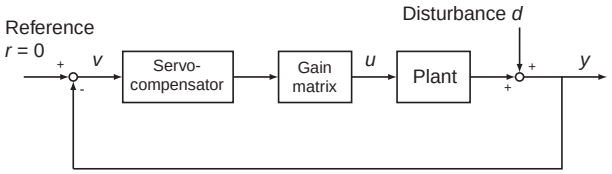

Fig. 6 Disturbance rejection control structure

described in the previous section. For each rotor, the number of outputs to be controlled is varied from three to six hub loads. The out-of-plane force and moments are chosen in the case of three hub loads. In the case of four outputs, the in-plane force F_x is added. In the case of five outputs, all three forces and the out-of-plane moments are considered. Finally, the entire force/moment vector at the rotor hub is considered when six outputs are controlled, see Table 2.

Table 2 Selection of outputs to be controlled

No. of	**3**	**4**	**5**	**6**
Selected Outputs	F_z, M_x, M_y	F_x, F_z, M_x, M_y	F_x, F_y, F_z, M_x, M_y	F_x, F_y, F_z, M_x, M_y, M_z

Table 3 shows the vibration reduction results for the different rotors and different numbers of outputs to be controlled. By following the first row of the table, a comparison can be made of the controllers designed for the same three outputs, but for different rotors. In all cases, the vibration in the outputs considered can be reduced considerably (between -96% and -91%). A slight degradation can be observed when a rotor with an increasing number of blades is considered in the design. This is due to the higher blade passage frequency and the assumption of identical actuator dynamics, which leads to a smaller gain and a larger phase lag in the frequency response of the actuators for an increasing number of blades.

Table 3 Vibration reduction results for different numbers of blades and outputs

Resulting Vibration[a]	**3-Blade Rotor**	**4-Blade Rotor**	**5-Blade Rotor**	**6-Blade Rotor**	**7-Blade Rotor**
3 Outputs	-96%	-94%	-93%	-92%	-91%
4 Outputs	-49%	-43%	-94%	-91%	-93%
5 Outputs	-23%	-20%	-92%	-88%	-92%
6 Outputs	-36%	-32%	-74%	-72%	-67%

a. Example reading: For the four-blade rotor, the vibration in the three considered outputs are reduced on average by -94% of the original values of the three outputs considered. The vibration reduction (or, possibly, the vibration increase) in the outputs not considered is not included in the number.

By taking into consideration the three-blade rotor and starting to increase the number of outputs to be controlled, the table shows that only three outputs can be reduced considerably. From four outputs onwards, the vibration can only be reduced by half of the original level (the shaded area in the table). A further increase in the number of outputs to be controlled further degrades vibration reduction. The results for the four-blade rotor are nearly identical to the results obtained with the three-blade rotor. The fourth blade does not lead to any additional degree of freedom being available for vibration control, since the rotor has a reactionless mode for an even number of blades. Thus, the vibration reduction potential is the same as it is for the three-blade rotor. The five and six-blade rotors allow a considerable vibration reduction (of between -92% and -88%) in five outputs. Although the results for up to five outputs are slightly better in the case of the seven-blade rotor, this rotor does not allow a considerable reduction in vibration (by around -90%) in all six forces/moments at the rotor hub, but only a value of -67% is achieved, which is a result comparable to the results of the five and six-blade rotors.

The result is that with three and four-blade rotors, three degrees of freedom are usable for vibration control, i.e. vibration can be reduced considerably in three outputs simultaneously. From five-blade rotors onwards, there are five degrees of freedom available for vibration reduction.

Singular Value Analysis of the Plant

The linear time-constant model of the helicopter rotor in MBC is analyzed in the following. The multi input multi output (MIMO) transfer function from the IBC inputs to the hub loads is analyzed using singular values. Fig. 7 shows the singular values for rotors with $N = 3$ to 7 blades. The frequency response is evaluated for a frequency from 1/rev to 10/rev. The number of singular values coincides with the number of inputs (number of rotor blades, inputs in MBC). A comparison of the singular values of the three-blade rotor with those of the four-blade rotor shows that the largest three singular values (collective, progressive, and regressive cyclic modes) are almost identical, whereas the additional degree of freedom in the four-blade rotor corresponds to the differential mode with a gain some -100dB lower (reactionless) than the other modes. In the case of five rotor blades, first and second-order cyclic modes exist, resulting in five "usable" modes for active rotor control. As is the case for the four-blade rotor, the differential mode of the six-blade rotor is reactionless. The third-order cyclic modes in the case of seven rotor blades have a gain some -50dB and -100dB lower than the collective and the first and second cyclic modes. From a control law design perspective, this basically leaves five modes available for rotor control, as is the case for the five and six-blade rotors.

The findings confirm the results of the previous section where the number of degrees of freedom was examined by designing controllers with an increasing number of outputs to be controlled.

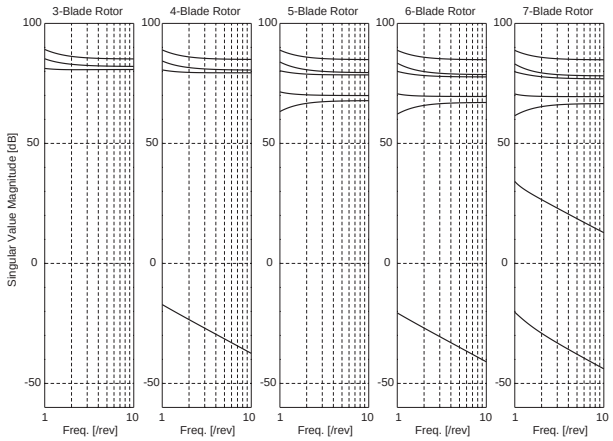

Fig. 7 Singular values of the *N*-blade rotors

Lag Damping Enhancement

In addition to reducing vibration at the blade passage frequency N/rev, a main objective of the control law design is to increase damping, especially in the weakly damped lag modes, in order to reduce gust sensitivity. This section examines the possibilities of lag damping from the nonrotating frame in more detail.

If the advantage of individual blade root control, namely the usability of unchanged blades, is to be exploited, control strategies without lag rate sensing in the rotating blades are required. Therefore, the control strategy for increasing damping is to use an observer-based controller and to feed back the (observed) rates of the modes to be controlled (Ref. 11). The physical mechanism of lag damping augmentation is as follows: The (observed) lag rate is fed back to the individual blade pitch control. A blade flapping rate is thus generated, which results in an in-plane moment due to the Coriolis force opposing the lag motion. Since the opposing Coriolis force is proportional to the lag rate, blade damping is augmented (Ref. 5).

By definition, the observer requires that the modes to be controlled are observable in the measured outputs. The differential lag mode cannot be controlled by a time-constant controller based on a time-constant approximation of the time-periodic plant, since the differential mode is not observable ("reactionless" mode) in the time-constant system.

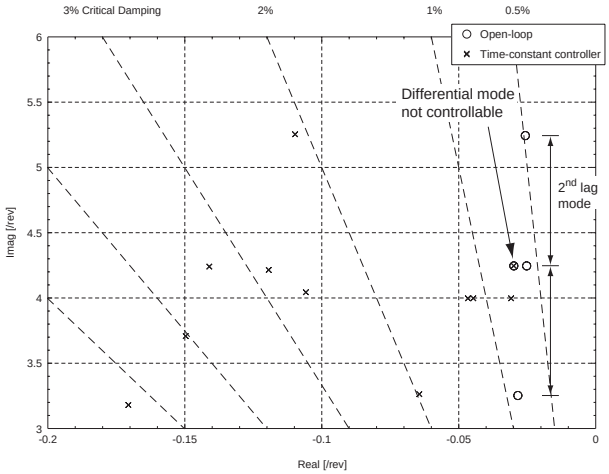

Fig. 8 Open-loop pole locations vs. closed-loop pole locations

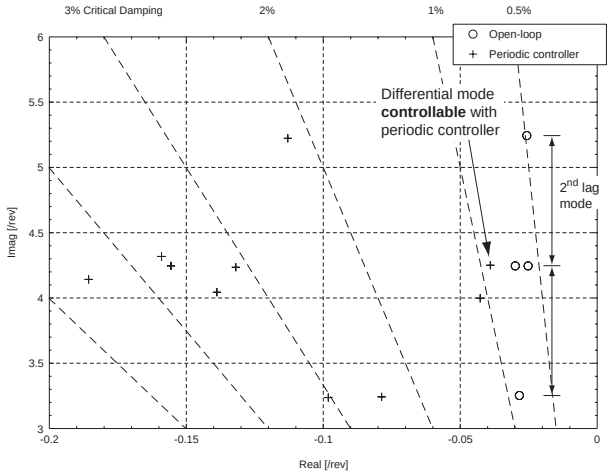

Fig. 9 Open-loop pole locations vs. closed-loop Poincaré exponents (closed-loop pole locations of the Floquet-transformed periodic system with time-periodic controller)

The section of the pole map containing the most relevant second lag mode is given in Fig. 8. The critical damping of the cyclic modes is increased from the minimum open-loop damping of 0.5% to 2% in the closed-loop. Collective lag mode damping is increased to >2%, assuming a measurement of M_z is available. The differential mode remains unchanged.

Fig. 9 shows the results for a time-periodic controller (Ref. 11). The controller is based on the same design parameters as above, with the exception of time-periodicity. The open-loop pole locations of the plant are compared with the Poincaré exponents (closed-loop pole locations of the Floquet-transformed time-periodic closed-loop system). While the results of the cyclic and collective modes are only slightly improved, the key result is that the time-periodic controller allows one to control the differential mode. Differential second lag mode damping is increased to approximately 1% critical damping. The possible differential damping enhancement is not as large as for the cyclic or collective form. This is due to the dynamic properties of the plant and not to periodicity or the gain-scheduled time-periodic implementation of the controller, since time-constant controller designs for fictitious time-constant rotors “fixed” at specific azimuthal positions yield similar results (Ref. 11). Although the differential damping enhancement is smaller than that for the cyclic and collective forms, the time-periodic controller allows one to increase second lag mode damping from minimal 0.5% critical damping to 1% in the differential form and to 2%-3% in the collective and cyclic form, whereas with a controller design based on the constant coefficient approximation, it is not possible to control the differential form from the nonrotating system.

Conclusion

This paper has addressed effects associated with the time-periodicity of the rotor and examined the interaction of the multiblade coordinate transformation, the multiharmonic response of the system, and the hub filtering effect of the rotor. The use of multiblade coordinates opens up the possibility to use time-constant control design techniques. However, the “reactionless” mode (for even blade numbers) can only be controlled using periodic control.

A simple analytical model for an N-blade rotor was developed and used to analyze the potential of individual blade control and examine its dependence on the number of rotor blades. The result is that the achievable vibration reduction depends on the available number of degrees of freedom, which in turn depends on the number of rotor blades. With three and four-blade rotors, three degrees of freedom can be used for vibration control. From five-blade rotors onwards, there are five degrees of freedom available for vibration reduction.

The capability of an observer-based control law to increase lag damping without dedicated blade sensors was demonstrated. The controller was applied in simulation to a complex model of a four-blade BO 105 helicopter rotor derived with the comprehensive aeromechanical helicopter and rotor analysis software Camrad II.

References

1. Bramwell, A. R. S, “Helicopter Dynamics”, Butterworth-Heinemann, ISBN 0-7506-5075-3, 2001
2. Cole, D. G., “Harmonic and Narrowband Distur-

bance Rejection for Linear Time-Periodic Plants", Dissertation, Virginia Polytechnic Institute and State University, Blacksburg, 1998

3. Davison, E. J., Furguson, I. J., "The Design of Controllers for the Multivariable Robust Servomechanism Problem Using Parameter Optimization Methods", IEEE Transactions on Automatic Control, AC-26(1), pp. 93-110, 1981
4. Dieterich, O., "Application of Modern Control Technology for Advanced IBC Systems", 24th European Rotorcraft Forum, Marseilles, 1998
5. Ham, N. D., Behal, B. L., McKillip Jr., R. M., "Helicopter Rotor Lag Damping Augmentation Through Individual-Blade-Control", Vertica, 7(4), pp. 361-371, 1983
6. Hohenemser, K. H., Sheng-Kuang Yin, "Some Applications of the Method of Multiblade Coordinates", Journal of the American Helicopter Society, 17(3), pp. 3-12,1972
7. Johnson, W., "CAMRAD II Comprehensive Analytical Model of Rotorcraft Aerodynamics and Dynamics", Johnson Aeronautics, Palo Alto, California, 1999
8. Johnson, W., "Helicopter Theory", Dover Publications, ISBN 0-486-68230-7, 1994
9. Kretz, M., Larché, M., "Future of Helicopter Rotor Control", Vertica, 4, pp. 13-22, 1980
10. Landmann, B., "Aufbau und Validierung eines Hubschrauberrotormodells", Diploma Thesis, University of Stuttgart, Institute of Flight Mechanics and Control, IFR_SR_00_003, 2000
11. Mannchen, T., Well, K. H., "Helicopter Vibration Reduction Using Periodic Robust Control", AIAA Guidance, Navigation and Control Conference, AIAA-2001-4034, Montreal, 2001
12. Moerder, D. D., Calise, A. J., "Convergence of a Numerical Algorithm for Calculating Optimal Output Feedback Gains", IEEE Transactions on Automatic Control, AC-30(9), pp. 900-903, 1985
13. Müller, M., Arnold, U.T.P., Morbitzer, D., "On the Importance and Effectiveness of 2/REV IBC for Noise, Vibration and Pitch Link Load Reduction", 25th European Rotorcraft Forum, Rome, 1999
14. Schwenger, M., "Hubschrauber-Vibrationsreduktion Reglerentwurf für eine unterschiedliche Anzahl der Rotorblätter", Diploma Thesis, University of Stuttgart, Institute of Flight Mechanics and Control, IFR_SR_01_017, 2001
15. Teves, D., Klöppel, V., Richter, P., "Development of Active Control Technology in the Rotating System, Flight Testing and Theoretical Investigations", 18th European Rotorcraft Forum, Avignon, 1992